Spatial Statistics 74 (2026) 100986

Contents lists available at ScienceDirect

Spatial Statistics

journal homepage: www.elsevier.com/locate/spasta

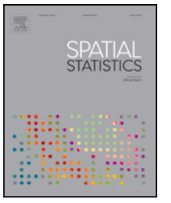

Local summary statistics for spatial point process intensity estimation ☆

Nicoletta D'Angelo [a],*, Giada Adelfio [a], Jorge Mateu [b], Ottmar Cronie [c]

[a] Department of Business, Economics and Statistics, University of Palermo, Palermo, Italy
[b] Department of Mathematics, University Jaume I, Castellon, Spain
[c] Department of Mathematical Sciences, Chalmers University of Technology and University of Gothenburg, Gothenburg, Sweden

ARTICLE INFO

Keywords:
Intensity estimation
Local characteristics
Poisson log-likelihood
Spatial point patterns
Summary statistics

ABSTRACT

Common practice in spatial point process modelling dictates that formal analysis begins with intensity estimation, which is carried out by exploiting external covariates, when available. Using this intensity estimate, one usually proceeds by obtaining non-parametric summary statistics estimates, in order to assess which model best fits the data. The state of the art in parametric intensity modelling is employing the Poisson likelihood function, but this underperforms when the data come from a more complex model, with some kind of interaction among points. Hence, to address this shortcoming, we propose a method that incorporates local second-order characteristics to account for spatial dependencies in the model fitting procedure. Our method relies on a locally weighted Poisson log-likelihood, which avoids making explicit assumptions about the type and degree of spatial interaction. We are therefore able to include external covariates while exploiting the non-parametric methods' advantages, flexibly including second-order characteristics. We further propose a non-parametric test for the detection of interaction between points. Simulation studies demonstrate that the proposed method outperforms standard approaches in capturing diverse spatial interaction behaviours. An application to real forestry data further highlights the model's flexibility in the presence of locally varying point interaction structures.

1. Introduction

When modelling point processes, a central aim is to fit a first-order intensity function to understand the overall rate of occurrence of points and how this changes across space and time. More specifically, one typically seeks to express the intensity function of the underlying point process as a function of available covariates. In the context of spatial point processes, for example, it may be suitable to assume a log-linear intensity function model depending on a set of spatial covariates, fitted under the assumption that the data come from a Poisson process. The description of real point processes, however, often requires more complex models than a Poisson process, since a Poisson process is based on the assumption of the absence of interdependence between events. Two large classes of alternative models for the analysis of spatial point patterns are Gibbs and Cox processes (Van Lieshout, 2000; Moller and Waagepetersen, 2003; Illian et al., 2008). Gibbs processes typically exhibit negative association, while Cox processes always exhibit positive association.

☆ This article is part of a Special issue entitled: 'SPASTA_dawn of AI' published in Spatial Statistics.

* Corresponding author.
E-mail address: nicoletta.dangelo@unipa.it (N. D'Angelo).

https://doi.org/10.1016/j.spasta.2026.100986
Received 25 November 2025; Received in revised form 9 March 2026; Accepted 2 April 2026
Available online 18 May 2026

A common first step in the analysis is therefore to assess the presence of clustering or inhibition in the point pattern, to further select an appropriate model family. This strategy, however, only captures the global behaviour of the pattern and may fail to properly guide the choice of the most suitable model. Most importantly, it disregards local interaction variations that may be crucial for model fitting. To address this issue, we propose a method that exploits the individual contribution of points to the second-order characteristics, to incorporate local dependencies into the intensity modelling.

Our method relies on a locally weighted Poisson process log-likelihood, avoiding the need to impose specific assumptions about the interaction structure or the degree of spatial interaction. Although weighted likelihood estimators have been proposed in the literature, they are generally limited to specific classes of models. For example, Zhuang (2015) proposed a weighted likelihood estimator for the space–time Epidemic Type Aftershocks Sequence (ETAS) model (Ogata, 1988) to study spatial variation in clustering features of seismicity in Japan, and Baddeley (2017) introduced weighted estimators for a wide class of spatial models. More recently, weighted likelihood and moment-based estimators have also been applied in spatio-temporal contexts (D'Angelo et al., 2023; D'Angelo and Adelfio, 2024a, 2025).

Our contribution extends beyond these previous works by proposing a general framework that maintains the interpretability of global model parameters, regardless of the actual data-generating process and intensity function. By flexibly adjusting for local interactions within the framework of Poisson process modelling, and by recalling that a Poisson process is completely specified by its intensity function, our method retains the interpretability and comparability of first-order intensity-based models. This enables the application of standard and well-established model assessment techniques across a broader class of point process models.

In particular, we adopt a semi-parametric modelling strategy in which the dependence structure among points is incorporated through appropriate weights derived from a local second-order interaction term. Specifically, we express the intensity function as the product of two components: a log-linear intensity function that may include the spatial covariates, and an interaction term that captures spatial dependence. This second component is estimated externally using local second-order summary statistics (D'Angelo et al., 2024), and then integrated into the likelihood function as a weight. The final estimation proceeds through a weighted Poisson process likelihood, where the weights correspond to a non-parametric estimate of the interaction term.

The interaction term can be estimated in several ways. In this work, we propose to base it on summary statistics such as the pair correlation function or the K-function, and in particular on their localised versions, known as Local Indicators of Spatial Association (LISA) functions (Anselin, 1995). They are defined as a set of functions that are individually associated with each one of the points of the point pattern, and can provide information about the local behaviour of the pattern. Applications of LISA functions range from the detection of features and clusters (Mateu et al., 2007; Moraga and Montes, 2011) to diagnostic (Adelfio et al., 2020), and more recently, to the fitting of point process models with space and space–time varying parameters (Baddeley, 2017; D'Angelo and Adelfio, 2024a). In this work, we employ LISA functions for general global model fitting for the first time.

A key advantage of our method is its ability to disentangle the contributions of first- and second-order characteristics, reducing identifiability issues that commonly arise in point process modelling. Indeed, spatial structures such as clustering can often be confounded with underlying trends, commonly captured by the first-order intensity function. To tackle this, we adopt a three-step estimation procedure, enabling a clearer attribution of model components and ensuring that the assumed first-order structure is explicitly incorporated in the estimation procedure.

Importantly, the use of local K-functions to estimate the interaction term introduces flexibility that would be difficult to achieve with a global Poisson model. While our method ultimately produces a single set of estimated parameters, the local weighting allows it to adapt to spatial heterogeneity in the point pattern. This means that clustering and inhibition can coexist within the same model, without needing to predefine a hybrid structure or fixing the scale at which such behaviour occurs, and possibly change. In many contexts, imposing a global interaction structure can be overly restrictive, and our method avoids this pitfall.

The rest of the paper is organised as follows. Section 2 provides preliminaries on spatial point processes. Section 3 introduces our methodological proposal, incorporating local second-order summary statistics into a weighted Poisson likelihood framework, and proposes a test for assessing the departure from the Poisson assumption. Simulation results are presented in Section 4, and the application to real forestry data is reported in Section 5. Section 6 concludes the paper.

2. Point process preliminaries

We consider a simple point process $X = \{x_i\}_{i=1}^{N}$ (Daley and Vere-Jones, 2007), with points x_i in a subset W of the two-dimensional Euclidean space $\mathbb{R}^2$, which is equipped with the Lebesgue measure $|A| = \int_A \mathrm{d}z$ for Borel sets $A \in \mathcal{B}(\mathbb{R}^2)$; a closed Euclidean r-ball around $x \in \mathbb{R}^2$ is denoted by $b[x, r] = \{y \in \mathbb{R}^2 : \|x - y\| \leq r\}$. Formally, X is a random element in the measurable space $\mathcal{N}$ of locally finite point patterns $\mathbf{x} = \{x_1, \ldots, x_n\}$, $n \geq 0$ (Van Lieshout, 2000). A point location in the two-dimensional plane is denoted by a lowercase letter such as u, and it can be specified by its Cartesian coordinates, i.e. $u = (u_1, u_2)$, in such a way that we do not need to mention the coordinates explicitly.

The kth-order Campbell theorem states that, for any non-negative function f on $(\mathbb{R}^2)^k$, we have that

$$\mathbb{E}\left[\sum_{x_1,\ldots,x_k \in X}^{\neq} f(x_1, \ldots, x_k)\right] = \int_{\mathbb{R}^2} \cdots \int_{\mathbb{R}^2} f(u_1, \ldots, u_k)\lambda^{(k)}(u_1, \ldots, u_k) \prod_{i=1}^{k} \mathrm{d}u_i,$$

where $\neq$ indicates that the sum is over n-tuples of distinct points of X. This essential result defines one of the main tools of point process theory, i.e., the *product densities* $\lambda^{(k)}$, $k \geq 1$. The arguably most important product densities are obtained for $k = 1$ and $k = 2$, called the *intensity function* λ and the *second-order product density* λ_2, respectively. In short, the intensity function gives the rate of

occurrence of events in the given region, and the second-order product density describes the joint infinitesimal probabilities of any two points of X.

Note that we can equivalently define the intensity function as

$$\lambda(u) = \lim_{|\mathrm{d}u|\to 0} \frac{\mathbb{E}[N(\mathrm{d}u)]}{|\mathrm{d}u|}$$

where $\mathrm{d}u$ is an infinitesimal region that contains the point u belonging to the analysed region W, $|\mathrm{d}u|$ is its area and $\mathbb{E}[N(\mathrm{d}u)]$ denotes the expected number of events in $\mathrm{d}u$. When the intensity is constant, the process is called homogeneous. In the inhomogeneous case, the intensity is not constant along the study area, thus depending on the spatial coordinate u. If all points of a point process are independent, then, under weak conditions, it is completely described by its intensity function $\lambda(u)$ (Daley and Vere-Jones, 2007), which is the case for a Poisson process. A general spatial log-linear intensity model, generalising both homogeneous and inhomogeneous models, can be expressed as

$$\lambda_{Pois}(u) = \lambda_{Pois}(u;\boldsymbol{\psi}) = \exp\{\psi_0 + \psi_1 Z_1(u) + \cdots + \psi_q Z_q(u)\} \quad \boldsymbol{\psi} \in \Psi \subseteq \mathbb{R}^q, u \in W \tag{1}$$

where $\mathbf{Z}(u) = \{Z_1(u), \ldots, Z_q(u)\}$ are q spatial covariates and $\boldsymbol{\psi} = (\psi_0, \psi_1, \ldots, \psi_q)$ contains the unknown parameters. The estimation of these parameters is typically carried out through the maximisation of the Poisson process log-likelihood, defined as

$$\log \mathrm{L}(\boldsymbol{\psi}) = \sum_{x_i \in \mathbf{x}} \log \lambda_{Pois}(x_i;\boldsymbol{\psi}) - \int_W \lambda_{Pois}(u;\boldsymbol{\psi}) du. \tag{2}$$

As already indicated, the inter-point interaction between events is quantified by a second-order moment characterisation, more specifically the second-order intensity function, defined as

$$\lambda_2(u,v) = \lim_{|\mathrm{d}u\|\mathrm{d}v|\to 0} \frac{\mathbb{E}[N(\mathrm{d}u)N(\mathrm{d}v)]}{|\mathrm{d}u \parallel \mathrm{d}v|}$$

where $u \neq v$. Several functional summary statistics can be used to study second-order characteristics of a point process and to measure dependence. Among those, the K-function (Ripley, 1976) quantifies second-order interactions, and its properties are well understood. When the process is stationary, i.e. when we consider a point process on all of $\mathbb{R}^2$ and its distribution does not change if we shift the process by some vector, the most commonly used estimator is introduced by Ripley (1976):

$$\hat{K}(r) = \frac{1}{\lambda^2 |W|} \sum_{i=1}^{N} \sum_{j \neq i} \mathbf{1}(\|u_i - u_j\| \leq r),$$

where the term $\|u_i - u_j\|$ denotes the Euclidean distance between two points of the point process inside the observation window, while $\mathbf{1}(\|u_i - u_j\| \leq r)$ is an indicator function that takes the value of 1 if the distance between the two points is less than or equal to the spatial lag r, and 0 otherwise. The expected value of the estimator for a homogeneous Poisson process is $K_{Pois}(r) = \pi r^2$, $r \geq 0$. Deviations of $\hat{K}(r)$ from its expectation may suggest clustering or inhibition. Indeed, when $\hat{K}(r) > K_{Pois}(r)$, the empirical curve is higher than the theoretical curve, indicating that a typical point has more neighbours than would be expected if the pattern were completely random. In such a case, we say that this is consistent with clustering. When $\hat{K}(r) < K_{Pois}(r)$, we say that the pattern is consistent with repulsion or inhibitive behaviour.

The inhomogeneous, or weighted, version is given by

$$\hat{K}_{\lambda}(r) = \frac{1}{|W|} \sum_{i=1}^{N} \sum_{j \neq i} \frac{\mathbf{1}(\|u_i - u_j\| \leq r)}{\hat{\lambda}(u_i)\hat{\lambda}(u_j)},$$

with $\hat{\lambda}(\cdot)$ a fitted first-order intensity function.

We next introduce the local version of the K-function (D'Angelo et al., 2024). This corresponds to the individual contribution of each point to the global summary statistics. The estimator associated with the ith event is

$$\hat{K}^i(r) = \frac{1}{\lambda^2 |W|} \sum_{j \neq i} \mathbf{1}(\|u_i - u_j\| \leq r),$$

while its inhomogeneous, or weighted, version is given by

$$\hat{K}^i_{\lambda}(r) = \frac{1}{|W|} \sum_{j \neq i} \frac{\mathbf{1}(\|u_i - u_j\| \leq r)}{\hat{\lambda}(u_i)\hat{\lambda}(u_j)}. \tag{3}$$

Knowing that the expectation of the K function is πr^2, it can be easily shown that the same expectation holds for the local version, henceforth denoted by $K_{pois}(r)$.

Local characteristics of this kind are commonly referred to as Local Indicators of Spatial Association (LISA) functions (Anselin, 1995), defined as a set of functions that are individually associated with each one of the points of the point pattern, and can provide information about the local behaviour of the pattern.

3. Locally-weighted Poisson point process model

With our proposal, we want to quantify the local clustering or inhibitive behaviour of the point pattern and to account for it in the model fitting procedure. Most importantly, we want to achieve this without making any assumptions about the underlying process nature nor by basing it on a global statement, which might lead to the choice of an improper model family. Given this, we propose the following semi-parametric intensity function

$$\lambda_\phi(u) = \nu(u)\phi(u, \mathbf{x}), \tag{4}$$

that allows for modelling both clustered and inhibitive point patterns. The *interaction term* $\phi(u, \mathbf{x})$ is a dependence adjustment with respect to a Poisson process with first-order intensity function of a general spatial log-linear Poisson model. Therefore, model (4) can be expressed as

$$\lambda_\phi(u) = \lambda_\phi(u; \boldsymbol{\theta}) = \nu(u; \boldsymbol{\theta})\phi(u, \mathbf{x}) = \exp\{\theta_0 + \theta_1 Z_1(u) + \cdots + \theta_q Z_q(u)\}\phi(u, \mathbf{x}).$$

Note that the first-order intensity parameters $\boldsymbol{\theta}$ differ from $\boldsymbol{\psi}$ of Eq. (1) due to the novel estimation procedure, which now includes also the estimation of the interaction term $\phi(u, \mathbf{x})$. For a Poisson process, $\phi(u, \mathbf{x}) = 1$, or equivalently $\lambda_\phi(u)$ is equal to $\nu(u)$. In such a case, the vector $\boldsymbol{\theta}$ approaches $\boldsymbol{\psi}$. We say that a model is attractive or repulsive if $\phi(u, \mathbf{x}) > 1$ or $\phi(u, \mathbf{x}) < 1$, respectively.

While the trend component $\nu(u)$ only depends on point locations, the interaction term also depends on the pattern configuration $\mathbf{x}$. An example is the pairwise interaction process, where the interaction term depends on the distance between pairs of points (Møller and Waagepetersen, 2003). In a constructed marked or functional marked framework, the interaction term might include information on characteristics of the points (D'Angelo et al., 2024; Ghorbani et al., 2021).

The approach to parametric intensity estimation typically found in the literature is to set $\hat{\phi}(u, \mathbf{x}) = 1$, regardless of the data-generating point process, and proceed as if one were dealing with a Poisson process, i.e. to find an estimate by maximising the Poisson log-likelihood (2). This approach is referred to as composite likelihood estimation (Guan, 2006). This assumption, however, becomes problematic if $\hat{\phi}(u, \mathbf{x})$ deviates significantly from 1, which implies that there are stronger interactions at large. By not adjusting the intensity for the intrinsic dependence structure, one runs the risk of overfitting (Cronie and Van Lieshout, 2018; Cronie et al., 2024). This can lead to an over-belief in the influence of covariates on the outcome of the point process.

Furthermore, adjusting for a specific dependence structure, when possible, requires the selection of a specific family of parametric models, a decision that may not be easy or even necessary, especially when our goal is to obtain only a parametric estimate of the intensity function, to understand the effects of covariates on the underlying point process. Note that the choice of a parametric model family to use for the intensity function commonly involves non-parametric analyses of inhomogeneous summary statistics (Cronie and Van Lieshout, 2015; Cronie et al., 2020; Iftimi et al., 2019). These analyses help to identify whether the underlying point process shows clustering, inhibition, or a completely random structure. These approaches, however, have limitations, as they often do not provide specific insights into the exact model family that would be most appropriate. Finally, these exploratory approaches often guide towards a class of models that disregard local variations that may be crucial for model fitting.

We thus propose a procedure to avoid the dependence on rigid assumptions on the interaction behaviour of points based on the global second-order summary statistics, while mitigating the possible identifiability issue between the first- and second-order characteristics. Our idea consists of a three-step procedure:

1. Find an estimate $\hat{\lambda}_{Pois}(u; \boldsymbol{\psi})$ of the unweighted intensity using the Poisson process likelihood function (2).
2. Find and estimate $\hat{\phi}(u, \mathbf{x})$ of the interaction term, using $\hat{\lambda}_{Pois}(u; \boldsymbol{\psi})$.
3. Fit the first-order intensity function $\hat{\lambda}_\phi(u; \boldsymbol{\theta})$, exploiting the interaction term $\hat{\phi}(u, \mathbf{x})$; recall (4).

Henceforth, we refer to $\phi(u, \mathbf{x})$ as $\phi(u)$, to ease the notation.

A note is in order. One of the crucial challenges of point process modelling is the possible identifiability issue between first- and second-order characteristics of the observed point patterns. This problem arises since spatial lack of aggregation of points in a point pattern may be either attributable to the intensity function, i.e. first-order effects, or interactions between points, i.e. second-order characteristics. Note that the unweighted Poisson process likelihood method interprets any aggregation of points as an effect of a high intensity when, in fact, it might partially come from underlying interaction, resulting in the aforementioned overfitting. In our approach, we address such an identifiability issue by capturing the local spatial structure of the point pattern at the second step of the fitting procedure. Specifically, we employ weighted LISA functions to quantify the clustering behaviour of the analysed point pattern. These LISA functions provide information on the underlying second-order structure of the point process, which is then integrated into the modelling procedure in the Poisson point process fitted in the final step, by means of a certain weighting procedure. This allows us to separate the estimation of the first-order intensity from second-order characteristics, effectively reducing the identifiability problem. The inclusion of this adjustment ensures that the estimation process better reflects the interaction structure of the data-generating point process.

3.1. Model estimation: Locally weighted Poisson log-likelihood

To fit the proposed model, we resort to maximisation of the weighted Poisson log-likelihood

$$\log \mathrm{L}(\boldsymbol{\theta}) = \sum_{x \in \mathbf{x}} \log(\nu(x; \boldsymbol{\theta})\hat{\phi}(x)) - \int_W \nu(u; \boldsymbol{\theta})\hat{\phi}(u)du. \tag{5}$$

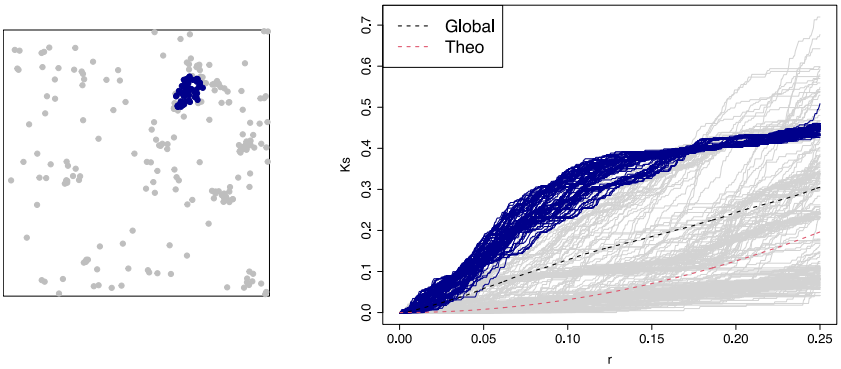

Fig. 1. Simulated clustered pattern with the most dense cluster indicated in blue (a) and the corresponding local K-function estimate (b). In black, the estimated global one. In red, the theoretical one when the underlying process is a Poisson process, i.e. $K_{Pois}(r)$. In grey, the estimated local ones. In blue, the local K-functions corresponding to the highlighted cluster.

By rewriting Eq. (5) as

$$\log \mathrm{L}(\boldsymbol{\theta}) = \sum_{x\in\mathbf{x}} \log \nu(x;\boldsymbol{\theta}) - \int_W \nu(u;\boldsymbol{\theta})\mathrm{d}u + \left[\sum_{x\in\mathbf{x}} \log \hat{\phi}(x) + \int_W \nu(u;\boldsymbol{\theta})(1-\hat{\phi}(u))\mathrm{d}u\right],$$

we see that it may be viewed as a regularised form of a Poisson log-likelihood, which is penalised by the amount of estimated interaction we have.

Note that to compute the integral in Eq. (5) we need the full surface $\{\hat{\phi}(u) : u \in W\}$. In practical terms, the optimisation of (5) is achieved by fitting

$$\lambda_\phi(u;\boldsymbol{\theta}) = \exp\{\theta_0 + \theta_1 Z_1(u) + \cdots + \theta_q Z_q(u) + \log[\hat{\phi}(u)]\},$$

to the data i.e. we introduce an external offset $\hat{\phi}(u)$, $u \in W$, into the model. This is very convenient, as it directly allows us to make use of efficient standard software for Poisson process intensity modelling, most notably the function `ppm.ppp` in the R (Team, 2025) package `spatstat` (Baddeley et al., 2015).

3.2. Discrepancy measures for the interaction term

Ideally, we expect a clustered process to have $\hat{\phi}(u) > 1$ on average, while for a Poisson process we aim to have $\hat{\phi}(u) = 1$, and $\hat{\phi}(u) < 1$ for an inhibitory process. Moreover, we also wish to capture local variations in the dependence structure, i.e. a structure varying in space. Therefore, we find it natural to make use of local summary statistics by employing the local weighted K-function (3).

Specifically, for any $x_i \in \mathbf{x}$, we let

$$\hat{\phi}(x_i) = \exp\{t(\hat{K}^i_\lambda(r), K_{Pois}(r))\} \tag{6}$$

with $t(\cdot,\cdot)$ a discrepancy measure quantifying the deviation between a local estimator of second-order characteristics of the analysed point pattern and its value under the Poisson process assumption. Formally, the discrepancy is a functional, taking two functions as inputs and providing a real number. Clearly, in (6), we want $t(f, f) = 0$ for any function f.

In order to have a better view on how to choose a sensible candidate for the discrepancy $t(\cdot,\cdot)$, Fig. 1 presents the estimated local K-functions of a simulated point pattern from a clustered point process.

More specifically, Fig. 1(a) shows a simulated clustered pattern with the most dense cluster indicated in blue; these represent the points for which we envision $\hat{\phi}(x_i)$ to be maximally distant from the constant value at 1. In Fig. 1(b), we show the corresponding local K-function estimates. In black, we report the estimated global one, i.e. the average of the local ones, in red, we depict the theoretical one when the underlying process is a Poisson process, $K_{Pois}(r)$, and in grey, we depict the estimated local ones. In blue, we highlight the local K-functions corresponding to the highlighted cluster, and the highlighted functions in turn. Therefore, we would like to find a discrepancy measure able to provide larger values of $\hat{\phi}(x_i)$ for the points in the highlighted cluster.

An intuitive proposal for $t(\cdot,\cdot)$ is the squared L_2 metric

$$t(\hat{K}^i_\lambda(r), K_{Pois}(r)) = \int_{r_0}^{r_{max}} sgn(\hat{K}^i_\lambda(r) - K_{Pois}(r))\left(\hat{K}^i_\lambda(r) - K_{Pois}(r)\right)^2 \mathrm{d}r, \tag{7}$$

adjusted by the sign of the difference, which is therefore able to discriminate between points showing a clustered or inhibitive behaviour. As a further option, we also consider

$$t(\hat{K}^i_\lambda(r), K_{Pois}(r)) = \int_{r_0}^{r_{max}} sgn(\hat{K}^i_\lambda(r) - K_{Pois}(r))\frac{(\hat{K}^i_\lambda(r) - K_{Pois}(r))^2}{K_{Pois}(r)}\mathrm{d}r. \tag{8}$$

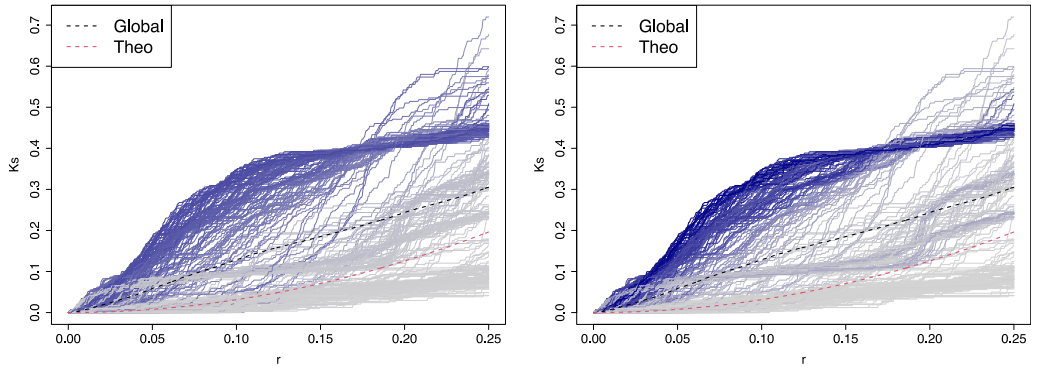

Fig. 2. Local K-functions, coloured by the estimated $\hat{\phi}(x_i)$ values. In panel (a), $t(\cdot,\cdot)$ is obtained through the squared difference of Eq. (7), and in panel (b), they are obtained by Eq. (8).

To visually assess whether a denser cluster renders higher values for $\hat{\phi}(x_i)$, we show the graph of the local K-functions, coloured by the estimated $\hat{\phi}(x_i)$ values in Fig. 2: the darker the colour, the higher the $\hat{\phi}(x_i)$ value. In particular, in Fig. 2(a), $t(\cdot,\cdot)$ is obtained through the squared difference of Eq. (7), while the values in Fig. 2(b) are obtained through (8).

We observe that the proposal in (8) better succeeds in assigning higher values of $\hat{\phi}(x_i)$ to the points of the highlighted cluster. This motivates us to consider the proposal in Eq. (8) rather than (7) for our study.

3.3. Interaction function interpolation

Regardless of the choice of discrepancy $t(\cdot,\cdot)$, in order to obtain an estimate $\hat{\phi}(u)$ for all locations $u \in W$, we need to use the collection $\{\hat{\phi}(x_i) : x_i \in \mathbf{x}\}$ to generate an interpolation $\{\hat{\phi}(u) : u \in W \setminus \mathbf{x}\}$.

There are different approaches to carrying out the spatial interpolation. Here, we focus on spatial smoothing of the numeric values observed at the point pattern locations, where

$$\hat{\phi}(u) = \frac{\sum_{i=1}^{n} \omega_i(u)\hat{\phi}(x_i)}{\sum_{i=1}^{n} \omega_i(u)},$$

given the estimates $\hat{\phi}(x_1), \dots, \hat{\phi}(x_n)$ at the points $\mathbf{x} = \{x_1, \dots, x_n\}$, together with a collection of suitable weight functions ω_i, $i = 1, \dots, n$.

The specific case of kernel weighting, using the Gaussian kernel κ, is achieved by letting $\omega_i(u) = \kappa(u - x_i)$. This yields the Nadaraya–Watson smoother (Nadaraya, 1964, 1989; Watson, 1964)

$$\hat{\phi}(u) = \frac{\sum_{i=1}^{n} \kappa(u - x_i)\hat{\phi}(x_i)}{\sum_{i=1}^{n} \kappa(u - x_i)}, \tag{9}$$

for any location $u \in W \setminus \mathbf{x}$. Here, the smoothing kernel bandwidth is chosen by least squares cross-validation for spatial smoothing with the `bw.smoothppp()` function of the `spatstat` R library (Baddeley and Turner, 2005).

An alternative is inverse-distance weighting (Shepard, 1968), where each weight is given by $\omega_i(u) = \|u - x_i\|^{-p}$, i.e. the inverse pth power of the Euclidean distance between u and x_i. Consequently, the smoothed value at u is given by

$$\hat{\phi}(u) = \frac{\sum_{i=1}^{n} \|u - x_i\|^{-p}\hat{\phi}(x_i)}{\sum_{i=1}^{n} \|u - x_i\|^{-p}}.$$

Fig. 3(a) shows the points of the simulated pattern, coloured by the estimated $\hat{\phi}(x_i)$ based on the discrepancy measure in (8). Panels (b) and (c) display the surfaces interpolated by the inverse-distance weighting and the kernel smoothing methods, respectively.

Throughout the paper, we employ the kernel smoother of Eq. (9), which generally provides smoother surfaces, a desirable property as it helps prevent overfitting.

3.4. Outline of the algorithm

After having selected the covariate dependence specification, the test function, and the smoothing methods, the outline of the procedure comes as follows.

1. Fit

$$\hat{\lambda}_{Pois}(u;\boldsymbol{\psi}) = \exp\{\hat{\psi}_0 + \hat{\psi}_1 Z_1(u) + \cdots + \hat{\psi}_q Z_q(u)\}$$

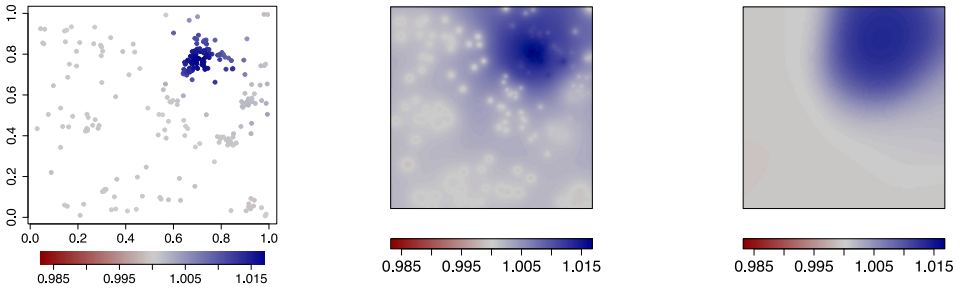

Fig. 3. Simulated pattern coloured by the estimated $\hat{\phi}(x_i)$ by the discrepancy measure in (8) (a), and their offsets $\hat{\phi}(u)$, $u \in W$, for the inverse-distance weighting with $p = 2$ (b), and kernel smoother with bandwidth equal to 0.13 (c) methods.

2. For any point in $\mathbf{x}$, compute

$$\hat{K}^i_\lambda(r) = \frac{1}{|W|} \sum_{j>i} \frac{\mathbf{1}(\|u_i - u_j\| \le r)}{\hat{\lambda}_{Pois}(u_i;\boldsymbol{\psi})\hat{\lambda}_{Pois}(u_j;\boldsymbol{\psi})}$$

3. For each point x_i, compute

$$\hat{\phi}(x_i) = \exp\left\{ \int_{r_0}^{r_{max}} sgn(\hat{K}^i_\lambda(r) - K_{Pois}(r)) \frac{(\hat{K}^i_\lambda(r) - K_{Pois}(r))^2}{K_{Pois}(r)} \mathrm{d}r \right\}$$

4. Smooth the surface

$$\hat{\phi}(u) = \frac{\sum_{i=1}^n \omega_i(u)\hat{\phi}(x_i)}{\sum_{i=1}^n \omega_i(u)},$$

5. Fit the final model, maintaining the same covariate dependence specification in $\hat{v}(u;\boldsymbol{\psi})$

$$\hat{\lambda}_\phi(u;\boldsymbol{\theta}) = \hat{v}(u;\boldsymbol{\theta})\hat{\phi}(u) = \exp\{\hat{\theta}_0 + \hat{\theta}_1 Z_1(u) + \cdots + \hat{\theta}_q Z_q(u) + \log[\hat{\phi}(u)]\}.$$

3.5. Testing for departure from the Poisson assumption

To test for the presence of interaction, we propose a statistical test based on the $\hat{\phi}(u)$ function. In particular, we test for *residual* interaction between points, after the overall trend is taken into account by the fitting of the first-order intensity in step 1 of the algorithm. Therefore, the system of hypothesis we wish to test is

$$\begin{cases} \mathcal{H}_0: & \text{The process is Poisson} \\ \mathcal{H}_1: & \text{The process is not Poisson.} \end{cases}$$

Under $\mathcal{H}_0$, the estimate of $\phi(u)$ should be close to $\phi_0(u) = 1$. Therefore, the statistical test comes as follows

$$\mathcal{T} = \int_W \log \hat{\phi}(u)\mathrm{d}u.$$

We approximate its null distribution by Monte Carlo simulation under a Poisson process with intensity $\hat{\lambda}(u,\boldsymbol{\psi})$. Specifically, we generate n_{sim} independent realisations. For each simulated point pattern, we then calculate the simulated test statistic yielding a Monte Carlo sample $\{\mathcal{T}^{(1)},\ldots,\mathcal{T}^{(n_{\text{sim}})}\}$. For a significance level α, the critical region can be defined according to the nature of the alternative hypothesis. For a two-sided alternative as above, we determine both critical values $c_{\alpha/2} = \text{quantile}_{\alpha/2}(\mathcal{T}^{(1)},\ldots,\mathcal{T}^{(n_{\text{sim}})})$, and $c_{1-\alpha/2} = \text{quantile}_{1-\alpha/2}(\mathcal{T}^{(1)},\ldots,\mathcal{T}^{(n_{\text{sim}})})$, and we reject the null hypothesis whenever $\mathcal{T}_{\text{obs}} < c_{\alpha/2}$ or $\mathcal{T}_{\text{obs}} > c_{1-\alpha/2}$. In contrast, when testing specifically for clustering or inhibition, i.e.

$$\begin{cases} \mathcal{H}_0: & \text{The process is Poisson} \\ \mathcal{H}_1: & \text{The process is clustered} \end{cases}$$

or

$$\begin{cases} \mathcal{H}_0: & \text{The process is Poisson} \\ \mathcal{H}_1: & \text{The process is inhibitory,} \end{cases}$$

a one-tailed criterion is used. In the case of a right-tailed or a left-tailed test, we compute the upper or lower critical value accordingly.

Table 1
Critical values of $\mathcal{T}$ for $\alpha = 0.05$ for a homogeneous Poisson process.

$\mathbb{E}[N]$	Critical values			
	c_{α}	$c_{1-\alpha}$	$c_{\alpha/2}$	$c_{1-\alpha/2}$
50	-1.73×10^{-3}	2.44×10^{-3}	-1.99×10^{-3}	3.66×10^{-3}
100	-8.09×10^{-4}	5.99×10^{-4}	-9.07×10^{-4}	9.10×10^{-4}
125	-5.97×10^{-4}	3.26×10^{-4}	-6.49×10^{-4}	4.90×10^{-4}
250	-2.80×10^{-4}	7.03×10^{-5}	-3.03×10^{-4}	1.00×10^{-4}
500	-1.28×10^{-4}	1.59×10^{-5}	-1.45×10^{-4}	3.48×10^{-5}

Table 2
Critical values of $\mathcal{T}$ for $\alpha = 0.05$ for a inhomogeneous Poisson process with intensity (10).

$\mathbb{E}[N]$	Critical values			
	c_{α}	$c_{1-\alpha}$	$c_{\alpha/2}$	$c_{1-\alpha/2}$
125	-9.04×10^{-4}	1.52×10^{-3}	-1.10×10^{-3}	2.01×10^{-3}
250	-4.00×10^{-4}	4.86×10^{-4}	-4.67×10^{-4}	6.41×10^{-4}
500	-1.96×10^{-4}	1.49×10^{-4}	-2.25×10^{-4}	2.15×10^{-4}

4. Simulation study

This section presents a simulation study to assess the performance of our proposed model in terms of goodness-of-fit. In particular, we are interested in understanding whether there is an improvement resulting from including the second-order characteristics in the first-order intensity function estimation, that is to say, using $\hat{\lambda}_{\phi}(u)$ instead of the composite likelihood choice based only on $\hat{\lambda}_{Pois}(u)$. Borrowing terminology from the framework of marked point processes, we are basically comparing the first-order intensity function identified by only the ground intensity, corresponding to $\hat{\lambda}_{Pois}(u)$, with the proposed intensity $\hat{\lambda}_{\phi}(u)$, which weights the ground intensity by the second-order characteristics information. We expect that the weighted likelihood leads to better fits when considering non-Poisson processes, capturing outlying second-order behaviour present in the point pattern.

4.1. Set-up

We here consider three model families, namely Poisson processes, LGCPs, and Strauss processes, since they represent, respectively, independence among points, clustering, and inhibition.

The performance is assessed by averaging over 1000 repetitions, in terms of the mean integrated squared error (MISE), given by

$$\mathrm{MISE}_{\hat{\lambda}} = \mathbb{E}\left[\int_{W} (\hat{\lambda}(u) - \lambda(u))^2 du\right].$$

Here $\lambda(u)$ denotes the intensity function of the generating process, X, henceforth called the *true* intensity function.

For both the Poisson processes and LGCPs, the form for $\lambda(u)$ is known explicitly, while for the Strauss process, in the same spirit as the smoothed raw residuals (Alm, 1998), we substitute the true intensity function by a non-parametric, kernel estimate of the intensity. The smoothing bandwidth is selected by cross-validation as the value that minimises the MSE criterion defined by Diggle (1985), by the method of Berman and Diggle (1989), to resemble the true intensity function the most. Furthermore, the Strauss model fits the conditional intensity function to the data, which we therefore numerically integrate to obtain the first-order intensity function and compute the MISE.

Since, for each scenario, $\hat{\lambda}_{\phi}(u) = \hat{v}(u)\hat{\phi}(u)$ is estimated, the interpolated surface $\hat{\phi}(u)$ is averaged over the spatial region and over the 1000 simulated patterns, and denoted by $\bar{\phi}$. We expect $\bar{\phi} \approx 1$ when we consider Poisson processes, and we expect it to deviate from 1 under the clustered and inhibitive scenarios, accordingly.

To further corroborate the significance of such results, we compute the rate of rejection of the test of departure from the Poisson assumption. The theoretical value of the statistical tests under the null hypothesis is obtained by computing the percentiles of the distribution of 1000 patterns simulated from Poisson point processes with expected number of points $\mathbb{E}[N]$. The obtained critical values employed throughout the simulation study are reported in Tables 1 and 2.

Throughout the study, we restrict the spatial domain to $W = [0, 1]^2$.

4.2. Poisson processes

In the first scenario, we consider homogeneous Poisson processes with constant intensity $\lambda \in \{125, 250, 500\}$, directly representing the expected number of points in $W = [0, 1]^2$.

We then examine inhomogeneous Poisson processes with a linear intensity function of the form

$$\lambda_{Pois}(u) = \lambda_{Pois}(u_1, u_2) = \psi_0 + 2u_2, \qquad (u_1, u_2) \in [0, 1]^2, \tag{10}$$

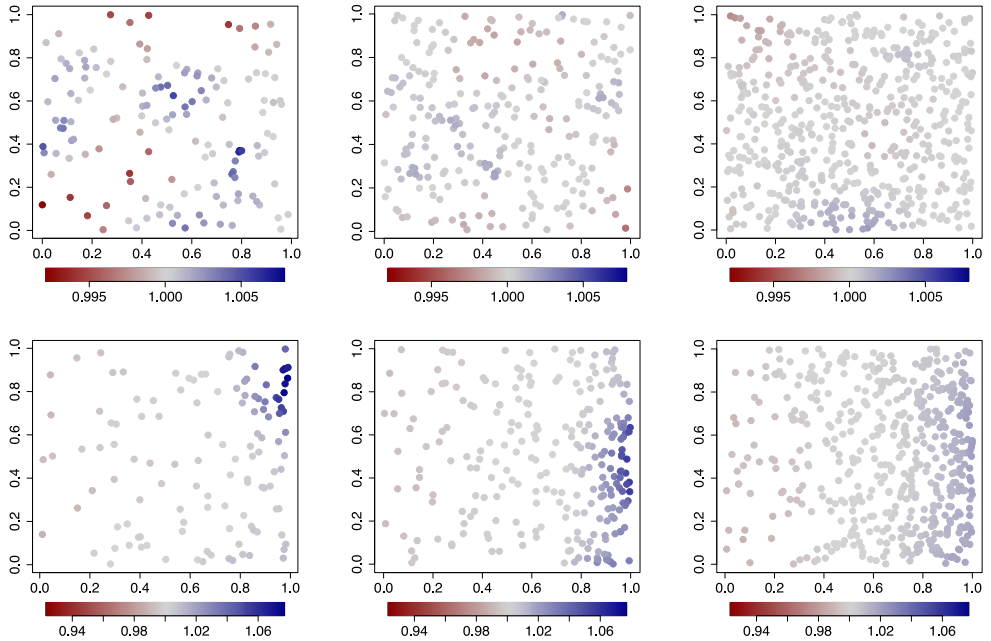

Fig. 4. Patterns simulated from Poisson processes. On the top panels, the processes have constant first-order intensity, while on the bottom panels, the true intensity function follows Eq. (10). The colour scale reflects the value of $\hat{\phi}(x_i)$.

Table 3
Results of the simulation study for the Poisson processes: MISE, $\bar{\phi}$, and type I error rates for the interaction test at $\alpha = 0.05$ over 1000 simulations.

Scenario	$\mathbb{E}[N]$	$\text{MISE}_{\hat{\lambda}_{Pois}}$	$\text{MISE}_{\hat{\lambda}_{\phi}}$	$\bar{\phi}$	Type I error rates
Homogeneous	125	2 159 739	2 160 938	0.9998	0.061
	250	4 261 200	4 262 485	0.9999	0.043
	500	8 565 015	8 566 446	0.9999	0.035
Inhomogeneous	125	302	302	1.0001	0.056
	250	558	558	0.9999	0.059
	500	1276	1276	0.9999	0.050

where (u_1, u_2) denotes the spatial coordinates explicitly. We let $\psi_0 \in \{3.67, 4.36, 5.05\}$, leading to having $\{125, 250, 500\}$ as expected numbers of points. Fig. 4 depicts realisations of these Poisson point processes with increasing number of points from left to right, while Table 3 reports the MISE, $\bar{\phi}$ values, and the type I error rates for the interaction test at $\alpha = 0.05$. We expect the proposed model to perform similarly to the benchmark Poisson.

As expected under the Poisson assumption, all three models yield very similar MISE values across different scenarios. Furthermore, the values of $\bar{\phi}$ are consistently close to 1 with rejection rates close to $\alpha = 0.05$, confirming that the proposed methods capture the independence structure of the Poisson processes. The slight deviations from 1 observed in some low-intensity cases (e.g., inhomogeneous Poisson with $\mathbb{E}[N] = 125$) are negligible and likely due to sampling variability, as shown in Fig. 4.

Overall, these results indicate that $\hat{\lambda}_{\phi}(u)$ performs comparably to the Poisson benchmark $\hat{\lambda}_{Pois}(u)$, without introducing spurious interaction, as reflected by the $\bar{\phi}$ indices being close to one.

4.3. Clustered processes

The next model family on which we evaluate our intensity estimation method is LGCPs. Following the inhomogeneous specification in Diggle et al. (2013), the LGCP for a generic point in space has the following random intensity

$$\Lambda(u) = \lambda(u) \exp(S(u))$$

where S is a Gaussian Random Field (GRF) with mean function $\mu = \mathbb{E}(S(u)) = -\frac{\sigma^2}{2}$ so that $\mathbb{E}[\exp(S(u))] = 1$. The covariance function is $\mathbb{C}(S(u), S(v)) = \mathbb{C}(\|u-v\|) = \sigma^2\rho(r)$ under the stationary assumption, i.e. it only depends on the variance parameter σ^2, the distance $r = \|u - v\|$ between locations u and v, and the correlation function of the GRF $\rho(\cdot)$. Specifically, let S be a Gaussian random field with zero mean and covariance function $\mathbb{C}(u, v) = \sigma^2 \exp(-\|u - v\|/\alpha)$, where σ^2 is the variance and α is the scale parameter for

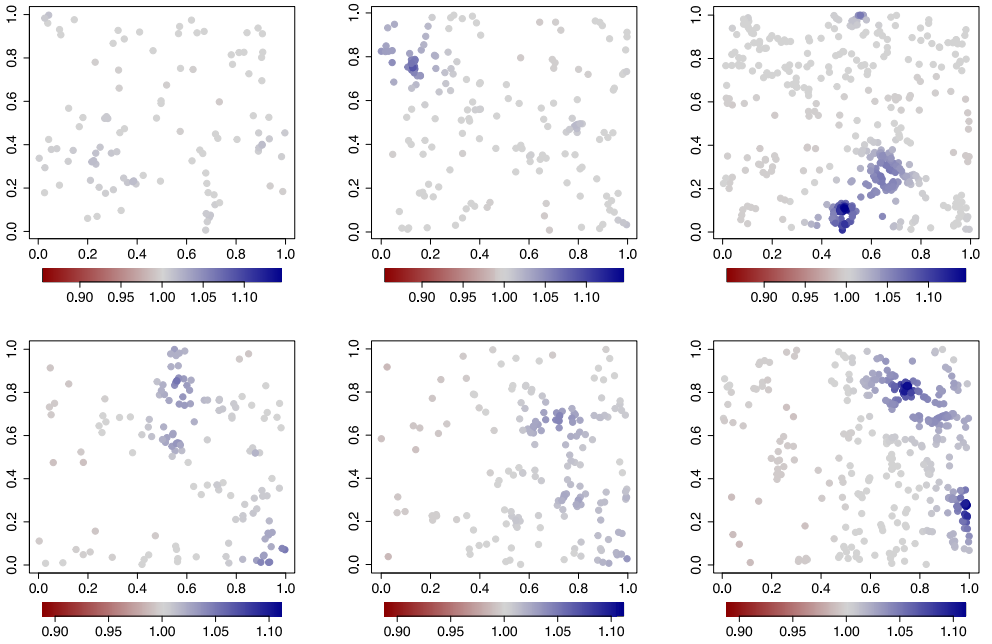

Fig. 5. Simulated patterns from LGCPs. On the top panels, the processes have constant first-order intensity, while on the bottom panels, the first-order intensity function follows Eq. (10). The colour scale reflects the value of $\hat{\phi}(x_i)$.

Table 4
Results of the simulation study for the LGCPs: MISE, $\bar{\phi}$, and power of the interaction test at $\alpha = 0.05$ over 1000 simulations.

Scenario	$\mathbb{E}[N]$	$\text{MISE}_{\hat{\lambda}_{LGCP}}$	$\text{MISE}_{\hat{\lambda}_{\phi}}$	$\text{MISE}_{\hat{\lambda}_{Pois}}$	$\text{MISE}_{\hat{\lambda}_{\phi}/\hat{\phi}}$	$\bar{\phi}$	Power
Homogeneous	125	63 697	658	6575	6359	1.0094	1.000
	250	249 100	2830	27 454	26 687	1.0081	1.000
	500	912 875	9763	105 221	102 603	1.0071	1.000
Inhomogeneous	125	163 486	19 037	9784	9531	1.0117	0.963
	250	614 482	79 666	38 536	37 680	1.0080	0.996
	500	2 630 759	334 645	158 013	154 648	1.0072	1.000

the spatial distance. This exponential form is widely used in this context and effectively reflects the distance-decaying correlation structure.

Consider further the random field defined by $\lambda_{Pois}\exp(S(u))$, which has a constant mean function. Then, the intensity function of the resulting Cox process, a homogeneous LGCP, is given by $\lambda_{LGCP} = \lambda_{Pois}\exp\{\sigma^2/2\}$. The first scenario here involves fixing σ^2 and α to 2 and 0.05, respectively, and letting λ_{Pois} and ψ_0 be $\{3.81, 4.50, 5.19\}$ and $\{2.65, 3.34, 4.03\}$ to obtain $\{125, 250, 500\}$ expected numbers of points. Table 4 reports the MISE, $\bar{\phi}$ and power of the interaction test at $\alpha = 0.05$ over 1000 simulations (see Fig. 5).

Turning to the more complex scenario of inhomogeneity combined with clustering, consider the random field $\lambda_{Pois}(u)\exp(S(u))$, with $\lambda_{Pois}(\cdot)$ strictly positive. Then, the resulting Cox process has an intensity function $\lambda_{LGCP}(u) = \lambda_{Pois}(u)\exp(\sigma^2/2)$. Here, we let $\lambda_{Pois}(u)$ be as in Eq. (10). Fig. 4 shows some realisations of LGCPs with an increasing number of points from left to right. On the top panels, the processes have constant first-order intensity, while on the bottom panels, the first-order intensity function follows Eq. (10). The associated intensity estimation results are given in Table 4.

In contrast to the Poisson case, the proposed method achieves consistently lower MISE values than the benchmark estimator $\hat{\lambda}_{LGCP}(u)$, across all scenarios and levels of expected number of points $\mathbb{E}[N]$. This reduction in MISE highlights the capacity of $\hat{\lambda}_{\phi}(u)$ to adapt to local spatial structures and to capture the additional variability induced by the latent Gaussian field, which the benchmark LGCP fails to model. Additionally, we compare the solely $\hat{\lambda}_{Pois}(u)$, which is estimated at the first step of the minimum contrast procedure for the LGCP model fitting, to our proposal intensity $\hat{\lambda}_{\phi}(u)$, divided by $\hat{\phi}(u)$. In this case the MISE is computed comparing the estimated intensities to the true intensity $\lambda_{Pois}(u)$, and not to $\lambda_{LGCP}(u) = \lambda_{Pois}(u)\exp(\sigma^2/2)$. We observe that the differences in MISE between our method and the benchmark are more evident when comparing the full first-order intensities. Conversely, neglecting the second-order characteristics results in a smaller reduction in MISE when using our method. This is likely because our method captures the second-order structure of the analysed pattern better than the cluster parameters of the LGCP, with the further advantage of a simpler semi-parametric estimation, compared to the minimum contrast method used in LGCPs.

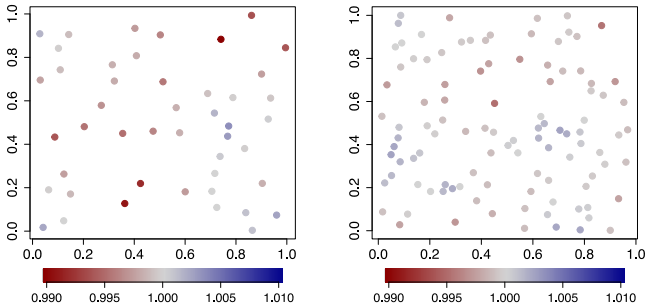

Fig. 6. Two point patterns simulated from Strauss processes with $\gamma = 0.1, \beta = 135,$ and $R = \{0.075, 0.03\}$, respectively. The colour scale reflects the value of $\hat{\phi}(x_i)$.

Table 5
Results of the simulation study for the Strauss processes: MISE, $\bar{\phi}$, and power of the interaction test at $\alpha = 0.05$ over 1000 simulations.

$\mathbb{E}[N]$	$\text{MISE}_{\hat{\lambda}_{Strauss}}$	$\text{MISE}_{\hat{\lambda}_{\phi}}$	$\bar{\phi}$	Power
50	665	662	0.9981	0.731
100	2097	2086	0.9993	0.301

The $\bar{\phi}$ values confirm this behaviour: they appear slightly above one in all scenarios, reflecting the presence of clustering. Their decrease as the number of points increases is likely due to the confounding between the inhomogeneity of the first-order trend and the second-order structure. However, the power of the test for $\alpha = 0.05$ is close to 1 for every scenario.

4.4. Inhibitive processes

Finally, we consider the Strauss process (Strauss, 1975; Kelly and Ripley, 1976; Ripley and Kelly, 1977) as an example of a model for spatial inhibition.

The Papangelou conditional intensity function is a fundamental concept for spatial point processes. Given a locally finite point configuration $\mathbf{x}$ and a location u, the Papangelou conditional intensity $\lambda(u|\mathbf{x})$ specifies the infinitesimal expected rate of finding a point at u, conditional on observing points at the locations given by $\mathbf{x}$. It is formally defined as $\lambda(u|\mathbf{x}) = f(\mathbf{x}|\{u\})/f(\mathbf{x})$ where $f(\cdot)$ is the density of the process with respect to a reference Poisson process.

For models specified via their Papangelou conditional intensity, the (unconditional) intensity function is typically intractable: often, it does not have a closed-form expression due to the complexity of the underlying interactions.

For instance, the conditional intensity of a Strauss process at a location u is available as

$$\lambda(u|\mathbf{x}) = \beta\gamma^{s(u,\mathbf{x})},$$

where $s(u, \mathbf{x})$ is the number of points of $\mathbf{x}$ lying within a distance R of location u, that is $s(u, \mathbf{x}) = \sum_{x_i \in \mathbf{x}} \mathbf{1}(\|u - x_i\| \leq R)$, β is a constant intensity parameter and γ is the interaction parameter.

This model depends on the value of the interaction parameter $\gamma \leq 1$ and the interaction radius R, such that each pair of points closer than R units apart contributes a factor γ to the density. Parameter γ regularises the inhibitive effect of the pattern: if $\gamma = 1$, the Strauss process reduces to a Poisson process; if $\gamma = 0$, the Strauss process is called a hard-core process with a hard-core radius $R/2$, since no pairs of points can lie closer than R units apart.

In this case, we generate 1000 realisations from Strauss processes with interaction parameter $\gamma = 0.1$ and $\beta = 135$. The interaction radius R is set to $\{0.075, 0.03\}$ to obtain patterns with $\{50, 100\}$ expected number of points. Fig. 6 depicts the simulated scenarios and Table 5 reports the results of the simulation study for the Strauss processes, that is, the MISE, $\bar{\phi}$ and power of the interaction test at $\alpha = 0.05$ over 1000 simulations. The benchmark $\hat{\lambda}_{Strauss}(u)$ is computed from the true conditional intensity function $\hat{\lambda}_{Strauss}(u) = \int_W \hat{\lambda}(u|\mathbf{x})\mathrm{d}\mathbf{x}$.

Also in this context, our proposed method yields lower MISE values compared to the benchmark, suggesting that it can capture the regularity of the pattern without requiring explicit knowledge of the underlying interaction model. Importantly, the $\bar{\phi}$ values are slightly below 1, reflecting the inhibitory nature of the process. The power of the test is quite high for $\mathbb{E}[N] = 50$ but decreases with the number of points. This is due to the departure from inhibition towards randomness when the number of points in a regular pattern increases, as evident from Fig. 6. These results confirm that our proposed model can flexibly adapt to regular point patterns, offering a good performance in settings with strong inhibition.

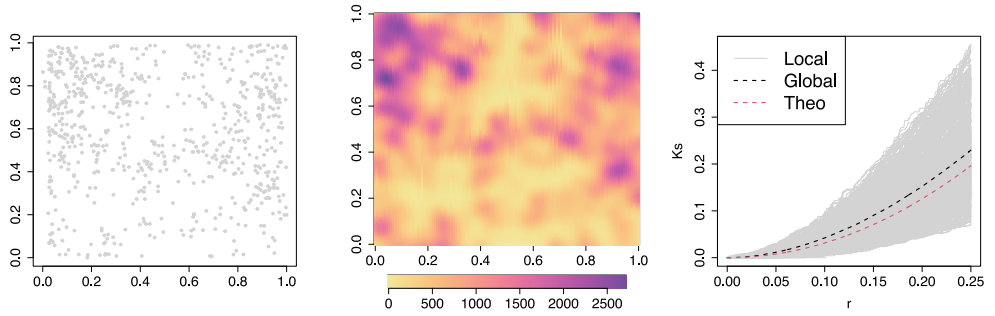

Fig. 7. Hickory tree point pattern (a) and its kernel intensity estimate (b). Estimated K-function of the Hickory trees point pattern (c).

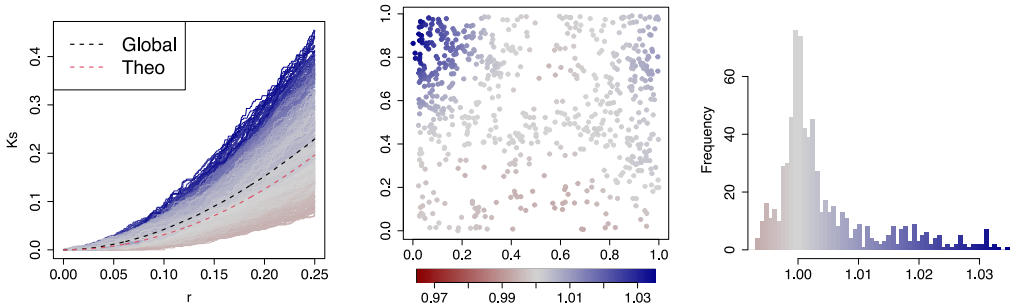

Fig. 8. Estimated K-functions of the Hickory trees point pattern (a). $\hat{\phi}(x_i)$ values of the Hickory trees pattern spatially displayed (b) and their distribution (c). The colour denotes the $\hat{\phi}(x_i)$.

5. Application

In this section, we analyse the locations of some botanical classifications of trees, found in the Lansing Woods dataset of the `spatstat` package (Baddeley and Turner, 2005).

The data come from an investigation of a 924 ft x 924 ft (19.6 acre) plot in Lansing Woods, Clinton County, Michigan USA supplied by D.J. Gerrard (Gerrard, 1969). Data consist of the locations of 2251 trees and their botanical classification (into hickories, maples, red oaks, white oaks, black oaks and miscellaneous trees). The original plot size (924 x 924 ft) has been rescaled to the unit square.

In particular, we selected the 703 hickory trees, depicted in Fig. 7(a). Fig. 7(b) displays a non-parametric estimate of the intensity fitted through a kernel procedure.

The spatial pattern appears to be strongly clustered in the upper left and right regions, and slightly regular in the bottom-centre region. Moreover, looking at the estimated global K-function of the pattern (black dashed line of Fig. 7(c)), we find clear indications of clustering. This indication is further confirmed by the global envelope test (Myllymäki et al., 2017) on Ripley's K-function, which resulted in a p-value < 0.05, leading to the rejection of the null hypothesis of complete spatial randomness (CSR). For this reason, a point process model tailored to clustering behaviour might be appropriate, and a possible candidate is an LGCP.

Looking at the local K-functions in Fig. 7(c), however, we observe some clear local differences in the behaviour of the points. This gives an indication that the global statement about the overall clustering behaviour of the pattern might be too restrictive, and therefore motivates us to develop a model that can take into account the local differences in the interaction behaviour of points within the pattern.

The curves under the Poisson line (red dashed curve) correspond to points inhibiting each other, while curves above the Poisson one correspond to clustered points (Fig. 8(a)). This is an indication that a global (clustered) model might not be appropriate for the analysed pattern. This is further confirmed by panels (b) and (c) of Fig. 8, which illustrate the $\hat{\phi}(x_i)$ values only at the point locations x_i and their empirical distribution.

Both the spatial display of such values and their distribution indicate an overall clustering behaviour of the observed pattern, with the majority of the points exhibiting $\hat{\phi}(x_i)$ values greater than one. In addition, this representation also enables us to pinpoint some points whose local structure is inhibitive, with values lower than one.

5.1. Model fitting

The covariance function parameters in the LGCP model offer insights into the clustering degree of the analysed pattern. Similarly, our proposed method facilitates an understanding of the dependence structure through the offset. Most importantly, the proposed method enables us to account for this aspect prior to model fitting.

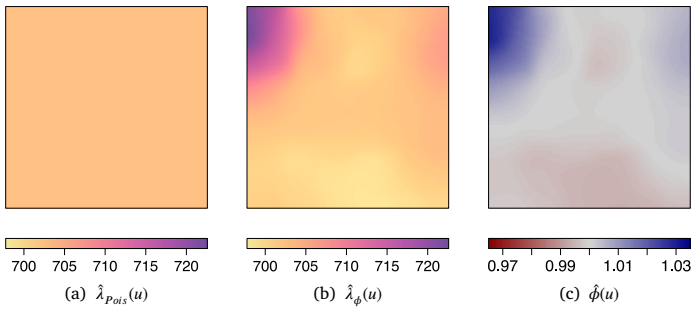

Fig. 9. The offset $\hat{\phi}(u)$, $u \in W$, and the intensities fitted for the Hickory trees pattern.

Table 6
MISE values of the four models fitted to the Hickory trees data.

	$\hat{\lambda}_{Pois}(u)$	$\hat{\lambda}_{Strauss}(u)$	$\hat{\lambda}_{LGCP}(u)$	$\hat{\lambda}_{\phi}(u)$
MISE	275 109	318 017	313 306	271 809

We first consider an LGCP model, with a constant first-order intensity function. Proceeding by fitting such a model by the minimum contrast procedure (Pfanzagl, 1969; Diggle and Gratton, 1984), the covariance function parameters are estimated to $\hat{\sigma}^2 = 0.50$ and $\hat{\alpha} = 0.13$, consequently resulting in a constant intensity $\hat{\lambda}_{LGCP} = \hat{\lambda}_{Pois} \exp(\hat{\sigma}^2/2)$ equal to 903. Note that $\hat{\lambda}_{Pois}$ is estimated to be 703.

Given that the pattern also displays some inhibitory behaviour, we fit a Strauss model with an interaction radius of $R = 0.27$. The fitted Strauss model yields a first-order term $\hat{\beta} = 528$, representing the baseline intensity of the process. The interaction strength is quantified by an estimated interaction parameter $\hat{\gamma} = 0.9995$, which is very close to one. Being non-significant, this parameter indicates an absence of interaction between points, indicating that the process does not deviate substantially from a homogeneous Poisson process (Baddeley et al., 2008; Coeurjolly and Rubak, 2013; Baddeley et al., 2016).

Then, we proceed by fitting the proposed weighted Poisson model with the following specification

$$\hat{\lambda}_{\phi}(u;\boldsymbol{\theta}) = \nu(\boldsymbol{\theta})\hat{\phi}(u) = \exp\{\hat{\theta}_0 + \log[\hat{\phi}(u)]\},$$

with $\hat{\nu}(\boldsymbol{\theta}) = \exp(\hat{\theta}_0) = 702$. Table 6 contains the MISE values for the fitted models. For an observed point pattern, of course, the true intensity in not known, so we substitute the true intensity function by a non-parametric, kernel estimate of the fitted intensity, with Berman and Diggle (1989)'s smoothing bandwidth.

The results show that the fitting method of the model improves when moving to a locally weighted fitting. Furthermore, the intensities resulting from the fitting of the Poisson model and from our proposed model are shown in Fig. 9(a),(b). Note that the locally-weighted Poisson point process model provides a non-constant fitted intensity function, basically resembling the fitted interaction term $\hat{\phi}(u)$ (Fig. 9(c)). Both the intensities fitted by the LGCP and the Strauss are constant as the Poisson one.

We underline that $\hat{\lambda}_{\phi}(u)$ obtains the best fit, and emphasise the importance of this discovery, namely the possibility of obtaining a smoothing strength typical of non-parametric methods while retaining all the advantages of parametric fitting. These include, for example, the possibility of obtaining an information criterion and the significance of the fitted parameters.

We highlight the importance of these results, as our proposal allows to quantify the local clustered or inhibitive behaviour of the point pattern and to account for it in the model fitting. Most importantly, this has been achieved without making any assumptions about the underlying process nature nor a global, somewhat limiting, statement.

Finally, for formally testing for departure from Poisson, we consider the test statistic 3.5 computed on the observed pattern, naming it $\mathcal{T}_{\text{obs}}$, which is equal to 1.04×10^{-3}. We approximate its null distribution by Monte Carlo simulation under a homogeneous Poisson process with intensity $\hat{\lambda}_{Pois}$, for a significance level $\alpha = 0.05$. Specifically, we generate $n_{\text{sim}} = 500$ independent realisations. The obtained critical values are: $c_{1-\alpha} = 7.88 \times 10^{-4}$, $c_{\alpha} = -6.55 \times 10^{-4}$, $c_{\alpha/2} = -9.64 \times 10^{-4}$, and $c_{1-\alpha/2} = 1.16 \times 10^{-3}$. Fig. 10 depicts the simulated test distribution obtained from 500 simulated homogeneous patterns with $\hat{\lambda}_{Pois}$ expected points, and informs us that the null hypothesis of the process being Poisson is rejected in favour of the alternative hypothesis stating that the process is clustered.

6. Conclusions

In this work, we have introduced a methodological framework that exploits local second-order statistics to enhance inference for complex intensity functions in spatial point processes. By incorporating spatial dependencies directly into the Poisson process intensity function, our method proves to be effective in adjusting for both clustering and inhibition features in the underlying point process. Through a simulation study and a real-data application, we have demonstrated the potential of our method to provide reliable parametric intensity estimates, particularly in scenarios where classical Poisson likelihood approaches may struggle, such as in the presence of complex local interaction structures.

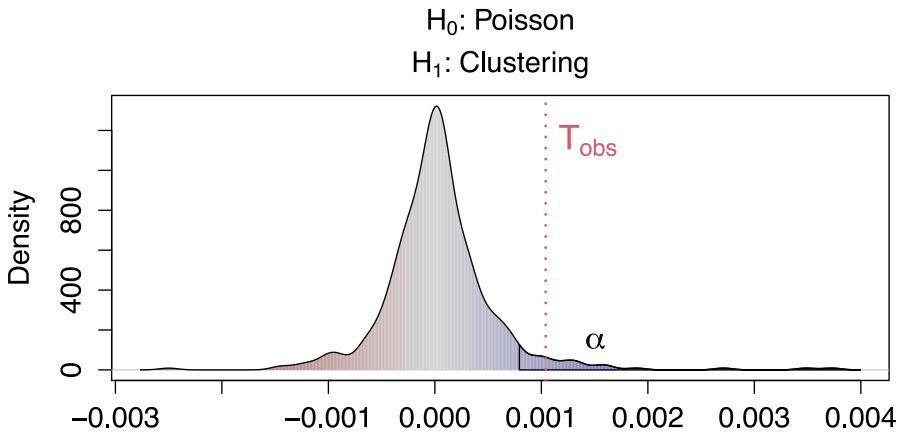

Fig. 10. Simulated test distribution obtained from 500 simulated patterns from a homogeneous Poisson process with $\hat{\lambda}_{Pois}$ expected points.

With our proposal, we have managed to quantify the local clustering or inhibitive behaviour of the point pattern and to account for it in the model fitting. Most importantly, we have been able to achieve this without making any assumptions about the underlying process nature or a global statement, which might lead to an improper model family, while still retaining competitive goodness-of-fit measures. A major advantage of our proposal is the ability to fit adaptively to the data in a non-parametric manner while retaining the possibility of estimating, and therefore interpreting, model parameters related to external spatial covariates. Furthermore, our contribution proposes a general framework that maintains the interpretability of global model parameters while allowing for direct comparisons across a broad range of models that provide first-order intensity functions. Finally, we propose a statistical test to assess departures from the Poisson assumption within the model fitting framework. Simulation results indicate that the test performs well in correctly identifying both the absence of interaction and the presence of clustering among points. As expected, its performance decreases in inhibitory scenarios, which are generally the most challenging to detect, as they tend to produce patterns that are less clearly distinguishable from the Poisson case.

A promising extension concerns the detection of changes in point pattern interaction structure, particularly when multiple behaviours coexist within the same study region. Techniques such as the classification of functional second-order characteristics (Adelfio et al., 2011; Sottile and Adelfio, 2019; González et al., 2021; D'Angelo et al., 2024) or spatial segmentation methods (D'Angelo, 2025a) could be applied to the estimated interaction term, enabling the identification of regions characterised by distinct clustering or inhibiting patterns, while retaining the flexibility of our modelling approach. Similarly, the scale at which such structures occur could be investigated by identifying change-points (Muggeo, 2003; Priulla and D'Angelo, 2024; D'Angelo, 2025b) in the discrepancy between observed K-functions and their expected values.

Even if our focus in this work is on the specification of clustering and inhibition structures, it is well recognised that the choice, transformation, and selection of covariates can be a major source of model misspecification in point pattern analysis. In practical applications, inadequate covariate specification may lead to biased or inefficient estimates of the intensity function, especially in inhomogeneous models where intensity is modelled as a function of spatial or spatio-temporal covariates. See, for instance, the recent development of regularised variable selection methods for Poisson point processes in Choiruddin et al. (2025). Methods such as penalised likelihoods, lasso or group lasso, and machine learning-based feature importance can help identify informative predictors while controlling for overfitting in high-dimensional settings. Including such considerations in model building can improve the interpretability and predictive performance of point process models.

Finally, although our methodology has been developed for point processes in Euclidean spaces, it can be naturally extended to non-Euclidean settings. For example, it can be applied to point processes on linear networks by incorporating local higher-order summary statistics as introduced by Cronie et al. (2020). Indeed, a further research direction involves extending our method to the spatio-temporal domain. The use of local spatio-temporal second-order summary statistics is becoming increasingly widespread as a means to capture interaction structures over both space and time. Notably, Siino et al. (2018) introduced the Local Indicators of Spatio-Temporal Association (LISTA) as a spatio-temporal extension of LISA functions, and Adelfio et al. (2020) later developed local versions of the (in)homogeneous spatio-temporal K-function, which can retain local features while serving as diagnostic tools. Such an extension could be operationalised through the cubature scheme recently proposed in D'Angelo and Adelfio (2025), which enables fitting Poisson point processes in three dimensions. This scheme is available in the R package `stopp` (D'Angelo and Adelfio, 2024b), hosted on the Comprehensive R Archive Network (CRAN), and provides a comprehensive framework for modelling spatio-temporal Poisson point processes.

Funding

The research work of Nicoletta D'Angelo and Giada Adelfio was supported by Fondi di Ateneo – Bando EUROSTART 2025 – progetto di ricerca ASPIRE – Advances in Spatio-temporal Point process models Innovations and Research, by the Targeted

Research Funds 2026 (FFR 2026) of the University of Palermo (Italy), and the PRIN 2022: Spatio-temporal Functional Marked Point Processes for probabilistic forecasting of earthquakes. P. I. Giada Adelfio CUP B53C24006340006. Ottmar Cronie was supported by the Swedish science council, Sweden (2023-03320) and Jorge Mateu was supported by the Ministry of Science and Innovatin, Spain (PID2022-141555OB-I00), and Generalitat Valenciana, Spain (CIAICO/2022/191).

References

Adelfio, G., Chiodi, M., D'Alessandro, A., Luzio, D., 2011. FPCA algorithm for waveform clustering. J. Commun. Comput. 8 (6), 494–502.
Adelfio, G., Siino, M., Mateu, J., Rodríguez-Cortés, F.J., 2020. Some properties of local weighted second-order statistics for spatio-temporal point processes. Stoch. Environ. Res. Risk Assess. 34 (1), 149–168.
Alm, S.E., 1998. Approximation and simulation of the distributions of scan statistics for Poisson processes in higher dimensions. Extremes 1 (1), 111–126.
Anselin, L., 1995. Local indicators of spatial association-LISA. Geogr. Anal. 27 (2), 93–115.
Baddeley, A., 2017. Local composite likelihood for spatial point processes. Spat. Stat. 22, 261–295.
Baddeley, A., Møller, J., Pakes, A.G., 2008. Properties of residuals for spatial point processes. Ann. Inst. Statist. Math. 60 (3), 627–649.
Baddeley, A., Rubak, E., Turner, R., 2015. Spatial Point Patterns: Methodology and Applications with R. Chapman and Hall/CRC Press, London.
Baddeley, A., Turner, R., 2005. spatstat: An r package for analyzing spatial point patterns. J. Stat. Softw. 12 (6), 1–42.
Baddeley, A., Turner, R., Rubak, E., 2016. Adjusted composite likelihood ratio test for spatial gibbs point processes. J. Stat. Comput. Simul. 86 (5), 922–941.
Berman, M., Diggle, P., 1989. Estimating weighted integrals of the second-order intensity of a spatial point process. J. R. Stat. Soc. Ser. B Stat. Methodol. 51 (1), 81–92.
Choiruddin, A., González, J.A., Mateu, J., Fadlurohman, A., Waagepetersen, R., 2025. Variable selection for spatio-temporal conditionally Poisson point processes. Comput. Statist. Data Anal. 212, 108238.
Coeurjolly, J.-F., Rubak, E., 2013. Fast covariance estimation for innovations computed from a spatial gibbs point process. Scand. J. Stat. 40 (4), 669–684.
Cronie, O., Moradi, M., Biscio, C.A., 2024. A cross-validation-based statistical theory for point processes. Biometrika 111 (2), 625–641.
Cronie, O., Moradi, M., Mateu, J., 2020. Inhomogeneous higher-order summary statistics for point processes on linear networks. Stat. Comput..
Cronie, O., Van Lieshout, M.N.M., 2015. AJ-function for inhomogeneous spatio-temporal point processes. Scand. J. Stat. 42 (2), 562–579.
Cronie, O., Van Lieshout, M.N.M., 2018. A non-model-based approach to bandwidth selection for kernel estimators of spatial intensity functions. Biometrika 105 (2), 455–462.
Daley, D.J., Vere-Jones, D., 2007. An Introduction to the Theory of Point Processes.Volume II: General Theory and Structure, second ed. Springer-Verlag, New York.
D'Angelo, N., 2025a. Detecting changes in space-varying parameters of local Poisson point processes. Environmetrics 36 (5), e70022.
D'Angelo, N., 2025b. Testing for a general changepoint in medical and psychometric studies: changes detection and sample size planning. Stat. Med. 44 (13–14), e70150.
D'Angelo, N., Adelfio, G., 2024a. Minimum contrast for the first-order intensity estimation of spatial and spatio-temporal point processes. Statist. Papers.
D'Angelo, N., Adelfio, G., 2024b. Stopp: Spatio-temporal point pattern methods, model fitting, diagnostics, simulation, local tests. R package version 0.2.4.
D'Angelo, N., Adelfio, G., 2025. Stopp: An r package for spatio-temporal point pattern analysis. J. Stat. Softw. 113, 1–35.
D'Angelo, N., Adelfio, G., Mateu, J., 2023. Locally weighted minimum contrast estimation for spatio-temporal log-Gaussian cox processes. Comput. Statist. Data Anal. 180, 107679.
D'Angelo, N., Adelfio, G., Mateu, J., Cronie, O., 2024. Local inhomogeneous weighted summary statistics for marked point processes. J. Comput. Graph. Statist. 33 (2), 588–602.
Diggle, P., 1985. A kernel method for smoothing point process data. J. R. Stat. Soc. Ser. C. Appl. Stat. 34 (2), 138–147.
Diggle, P.J., Gratton, R.J., 1984. Monte Carlo methods of inference for implicit statistical models. J. R. Stat. Soc. Ser. B Stat. Methodol. 46 (2), 193–212.
Diggle, P.J., Moraga, P., Rowlingson, B., Taylor, B.M., et al., 2013. Spatial and spatio-temporal log-Gaussian cox processes: extending the geostatistical paradigm. Statist. Sci. 28 (4), 542–563.
Gerrard, D.J., 1969. Competition Quotient: a New Measure of the Competition Affecting Individual Forest Trees, vol. 20, Agricultural Experiment Station, Michigan State University.
Ghorbani, M., Cronie, O., Mateu, J., Yu, J., 2021. Functional marked point processes: a natural structure to unify spatio-temporal frameworks and to analyse dependent functional data. Test 30 (3), 529–568.
González, J.A., Rodríguez-Cortés, F.J., Romano, E., Mateu, J., 2021. Classification of events using local pair correlation functions for spatial point patterns. J. Agric. Biol. Environ. Stat. 26 (4), 538–559.
Guan, Y., 2006. A composite likelihood approach in fitting spatial point process models. J. Amer. Statist. Assoc. 101 (476), 1502–1512.
Iftimi, A., Cronie, O., Montes, F., 2019. Second-order analysis of marked inhomogeneous spatiotemporal point processes: Applications to earthquake data. Scand. J. Stat. 46 (3), 661–685.
Illian, J., Penttinen, A., Stoyan, H., Stoyan, D., 2008. Statistical Analysis and Modelling of Spatial Point Patterns, vol. 70, John Wiley & Sons.
Kelly, F., Ripley, B., 1976. On strauss's model for clustering. Biometrika 63, 357–360.
Mateu, J., Lorenzo, G., Porcu, E., 2007. Detecting features in spatial point processes with clutter via local indicators of spatial association. J. Comput. Graph. Statist. 16 (4), 968–990.
Moller, J., Waagepetersen, R.P., 2003. Statistical Inference and Simulation for Spatial Point Processes. CRC Press.
Møller, J., Waagepetersen, R.P., 2003. Statistical Inference and Simulation for Spatial Point Processes. Chapman and Hall/CRC, Boca Raton.
Moraga, P., Montes, F., 2011. Detection of spatial disease clusters with LISA functions. Stat. Med. 30 (10), 1057–1071.
Muggeo, V.M., 2003. Estimating regression models with unknown break-points. Stat. Med. 22 (19), 3055–3071.
Myllymäki, M., Mrkvička, T., Grabarnik, P., Seijo, H., Hahn, U., 2017. Global envelope tests for spatial processes. J. R. Stat. Soc. Ser. B Stat. Methodol. 79 (2), 381–404.
Nadaraya, E.A., 1964. On estimating regression. Theory Probab. Appl. 9 (1), 141–142.
Nadaraya, E.A., 1989. Nonparametric Estimation of Probability Densities and Regression Curves. Springer.
Ogata, Y., 1988. Statistical models for earthquake occurrences and residual analysis for point processes. J. Amer. Statist. Assoc. 83 (401), 9–27.
Pfanzagl, J., 1969. On the measurability and consistency of minimum contrast estimates. Metrika 14 (1), 249–272.
Priulla, A., D'Angelo, N., 2024. Sequential hypothesis testing for selecting the number of changepoints in segmented regression models. Environ. Ecol. Stat. 31 (2), 583–604.
Ripley, B.D., 1976. The second-order analysis of stationary point processes. J. Appl. Probab. 13, 255–266.
Ripley, B.D., Kelly, F.P., 1977. Markov point processes. J. Lond. Math. Soc. 15, 188–192.
Shepard, D., 1968. A two-dimensional interpolation function for irregularly-spaced data. In: Proceedings of the 1968 23rd ACM National Conference. pp. 517–524.
Siino, M., Rodríguez-Cortés, F.J., Mateu, J., Adelfio, G., 2018. Testing for local structure in spatiotemporal point pattern data. Environmetrics 29 (5–6), e2463.
Sottile, G., Adelfio, G., 2019. Clusters of effects curves in quantile regression models. Comput. Statist. 34 (2), 551–569.
Strauss, D., 1975. A model for clustering. Biometrika 62, 467–475.
Team, R.C., 2025. R: A Language and Environment for Statistical Computing. R Foundation for Statistical Computing, Vienna, Austria.
Van Lieshout, M., 2000. Markov Point Processes and Their Applications. World Scientific.
Watson, G.S., 1964. Smooth regression analysis. SankhyĀ: Indian J. Stat. Ser. A 359–372.
Zhuang, J., 2015. Weighted likelihood estimators for point processes. Spat. Stat. 14, 166–178.